

# Nano-Sustained CO-Releasing Molecules Alleviates Cyclosporin-A-Induced Nephrotoxicity and Renal Fibrosis by Inhibiting *NLRP3* Inflammasome-Mediated TGF- $\beta$ /Smad Signaling Pathway

Juan Ji<sup>1†</sup>, Zhaoyu Bi<sup>1†</sup>, Ling Tian<sup>1</sup>, Qian Zhang<sup>2</sup>, Shu-fen Hou<sup>2</sup>, Song Li<sup>2\*</sup>

<sup>1</sup>Department of Nephrology, Affiliated Hospital of Hebei University, Baoding 071000, Hebei Province, China

<sup>2</sup>Department of Urology, Affiliated Hospital of Hebei University, Baoding 071000, Hebei Province, China

<sup>†</sup>These authors contributed equally to this work

\*Corresponding author: Song Li, 15830201177@sina.com

**Copyright:** © 2023 Author(s). This is an open-access article distributed under the terms of the Creative Commons Attribution License (CC BY 4.0), permitting distribution and reproduction in any medium, provided the original work is cited.

**Abstract:** *Objective:* To investigate the effect nano-sustained CO-releasing molecules on cyclosporin-A (CsA)-induced nephrotoxicity by inhibiting the *NLRP3* inflammasome-mediated TGF- $\beta$ /Smad signaling pathway. *Methods:*  $3 \times 10^5$  cell/mL human renal tubular epithelial cells (HK-2) and mouse primary cultured renal tubular epithelial cells (RTECs) were cultured under an inverted microscope and incubated with 10% DMEM and 0.25%  $\beta$ 2M in NaCl solution for 3 h. HK-2 and RTECs were divided into 5 complex numbers. MTT assay was used to detect the relative proliferation level of one of the HK-2 cells and calculate the multiplication ratio. *Results:* The nano-sustained CO-releasing molecules CS-CO had a strong protective effect on the kidney. HK-2 and RTECs cells were treated with siRNA, inhibitors, and *NLRP3* knockout mice, and the changes in cell activity and expression of intracellular inflammatory factors were studied. The expression of TGF- $\beta$ 1/Smad signaling pathway related proteins in HK-2 and RTECs was detected by ELISA, western blot, immunofluorescence, and other techniques. *Conclusion:* SMA/CORM2 alleviates CsA-induced renal fibrosis by inhibiting *NLRP3* inflammasome-mediated TGF- $\beta$ /Smad signaling pathway.

**Keywords:** *NLRP3*; TGF-beta; Smad; Renal fibrosis

**Online publication:** May 31, 2023

## 1. Introduction

*NLRP3* inflammasome activation is a major cause of renal inflammatory response in rat models of cyclosporine A (CsA)-induced renal fibrosis. Therefore, inhibition of *NLRP3* inflammasome activation is of great significance in alleviating CsA-induced renal fibrosis. Nano-sustained CO-releasing molecules (CS-CO) is a novel drug-carrying CO-releasing molecule, which plays an anti-inflammatory role *in vivo*. Our previous studies have shown that CS-CO can effectively inhibit the activation of *NLRP3* inflammasome in rat renal tissue, and blocking the activation of *NLRP3* inflammasome can alleviate CsA-induced renal fibrosis. In this study, rat renal tubular epithelial cells (RTECs) and human renal tubular epithelial cells (HK-2) were cultured to obtain renal tubular epithelial cells, renal tubule interstitium, and renal fibrosis models. siRNA, and *NLRP3* knockout mice were used, and then the changes in cell activity were detected. The activation of *NLRP3* inflammasome and the expression of inflammatory factors in HK-2 cells and

RTECs were observed by fluorescence staining. The plasma protein levels of HK-2 cells and RTECs were detected by western blotting. Fibroblast culture was treated with siRNA in *NLRP3* knockout mice, respectively, and the expression of TGF- $\beta$ 1/Smad signaling pathway related proteins was detected. A mouse model of renal fibrosis with *NLRP3* gene knockout was constructed, which confirmed that inhibition of *NLRP3* gene knockout can effectively alleviate the progression of CsA-induced renal fibrosis [1-5].

## 2. Information and methods

### 2.1. Materials

Non-stress responsive male rats of  $\geq 1000$ g were used as lab rats. The main instruments and equipment are biochemical analyzer, cell culture kit (ViralSystems, USA). The cell lysis solution was purchased from Beijing Dinghao Biotechnology Co Ltd. The petri dishes with were rinsed with sterile water at least 3 times to remove white blood cells and then with 0.1% benzyl ammonium chloride solution 2 times to remove dead cells. 10% HNO<sub>3</sub> (2mL/L) was used to prepare the buffer solution and 5% HNO<sub>3</sub> (2mL/L) was used to prepare PBS solution.

### 2.2. Main reagents

MTT kit (Shanghai Boosays Biotechnology Co., Ltd.), SDS-PAGE gel electrophoresis instrument (JC16Y1, USA) was for quantitative detection of protein expression.

Other reagents: 5% PBS buffer solution (pH 6.8), DAPI reagent, SDS gel preparation kit (Beijing Bosyes Company), CCK-8 solution (10  $\times$  cell adhesion method/PBS solution), Transwell cell culture medium and Transwell agarose gel column, BSA solution, 5% fetal bovine serum and 10 $\times$ PBS buffer solution, and cytokines (human interleukin-2, type 1, IL-10,IL-1,IL-12 and IL-6 [ELISA method], etc.) were prepared.

### 2.3. Methods

- (1) HK-2 and RTECs cell cultures:  $3 \times 10^5$  cell/mL Human renal tubular epithelial cells (HK-2) with and primary cultured mouse renal tubular epithelial cells (RTECs) were cultured under an inverted microscope and incubated with 10% DMEM and 0.25%  $\beta$ 2M in NaCl solution for 3h.
- (2) Experimental grouping: The ratio of the experimental groups and control groups were 1:1
- (3) Cell count: 1 mL human kidney tissue specimens were collected and stored in 1 mmol/L chloroform epoxide at the concentration of  $1 \times 10^5$  cells/mL.
- (4) Cell activity detection: HK-2 and RTECs cells were divided into 5 complex numbers. MTT assay was used to detect the relative proliferation level of one of the cells and calculate the multiplication factor.
- (5) Fluorescence staining (0.1 MPBS): Fibroblasts were divided into three complex numbers: blank control group, experimental group, and model group, and cultured for 1 hour in 1 mmol/L chloroform.
- (6) Western blotting: The proteins were detected by the western blot method.
- (7) Serum sample treatment: Serum samples were collected from animals in each group at different time points.
- (8) Statistical analysis: *NLRP3* protein expression in renal tubule epithelial cells was determined by immunohistochemical methods.
- (9) Calculation of the degree of renal fibrosis: Luminex kit was used to detect the degree of renal fibrosis of rats in each group, and Microsoft Excel was used for statistical processing (including curve plotting and analysis).

### 3. Results

#### 3.1. SMA/CORM2 alleviated CsA-induced renal pathological and histological changes

In order to investigate the effect of SMA/CORM2 on renal fibrosis, a CsA-induced renal fibrosis model and a SMA/CORM2 intervention model were first established (**Figure 1A**). Subsequently, we found that different doses of SMA/CORM2 improved CsA-induced renal weight loss and renal coefficient decrease, increased serum creatinine (Cr), and increased blood urea nitrogen (Bun) in male rats (**Figure. 1B-E**). It should be noted that 1 mg/kg SMA/CORM2 showed the most significant protective effect. Therefore, we will select 1 mg/kg SMA/CORM2 as the intervention dose in the following study.

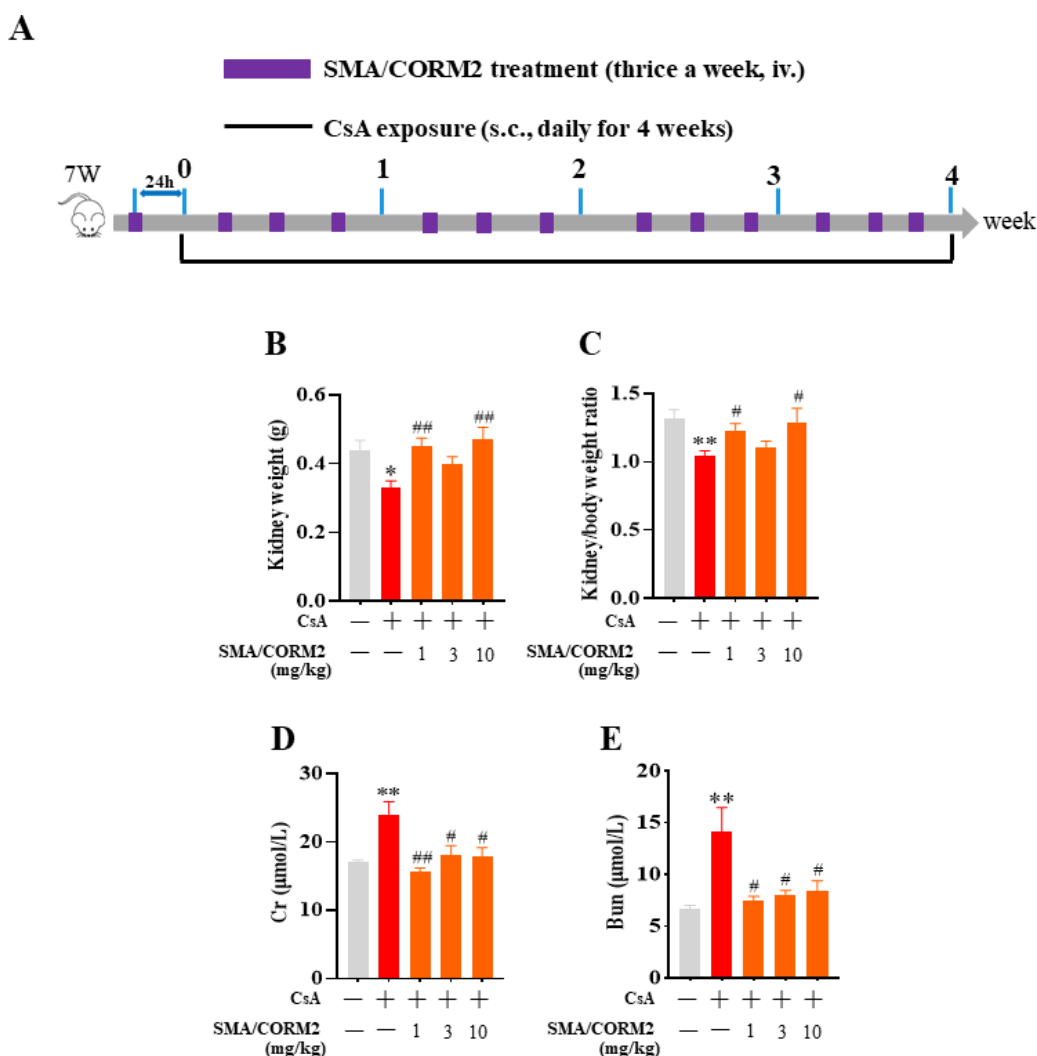


**Figure 1.** Effect of SMA/CORM2 on CsA- induced nephrotoxicity. (A) Experimental design; Mice were injected subcutaneously with CsA every day for 4 weeks, during which SMA/CORM2 was injected three times a week through the caudal vein. 24 hours after the last CsA injection, the mice were killed, and their renal weights were weighed. (B) Kidney weight. (C) Kidney/body weight ratio. (D) Serum creatinine. (E) blood urea nitrogen. \* $P < 0.05$ , \*\* $P < 0.01$  vs control group; # $P < 0.05$ , ### $P < 0.01$  vs CsA group. The results were expressed by mean  $\pm$  standard error,  $n \geq 4$ .

As shown in **Figure 2E-F**, H&E staining showed that CsA significantly damaged the tubular structure and aggravated the renal injury, which was manifested as increased necrotizing debris in the tubular, blurred tubular boundary and inflammatory cell infiltration, and increased tubular injury score. However, SMA/CORM2 significantly reversed this phenomenon. At the same time, we also evaluated the intervention effect of CORM2, as shown in **Figures 2A-D**. Although CORM2 can improve the decrease of

kidney weight, renal coefficient, serum creatinine (Cr) and blood urea nitrogen (Bun) induced by CsA in male rats, it was less effective than SMA/CORM2. As shown in **Figures 2E-F**, CORM2 also had a lower protective effect than SMA/CORM2 on tubular structure.

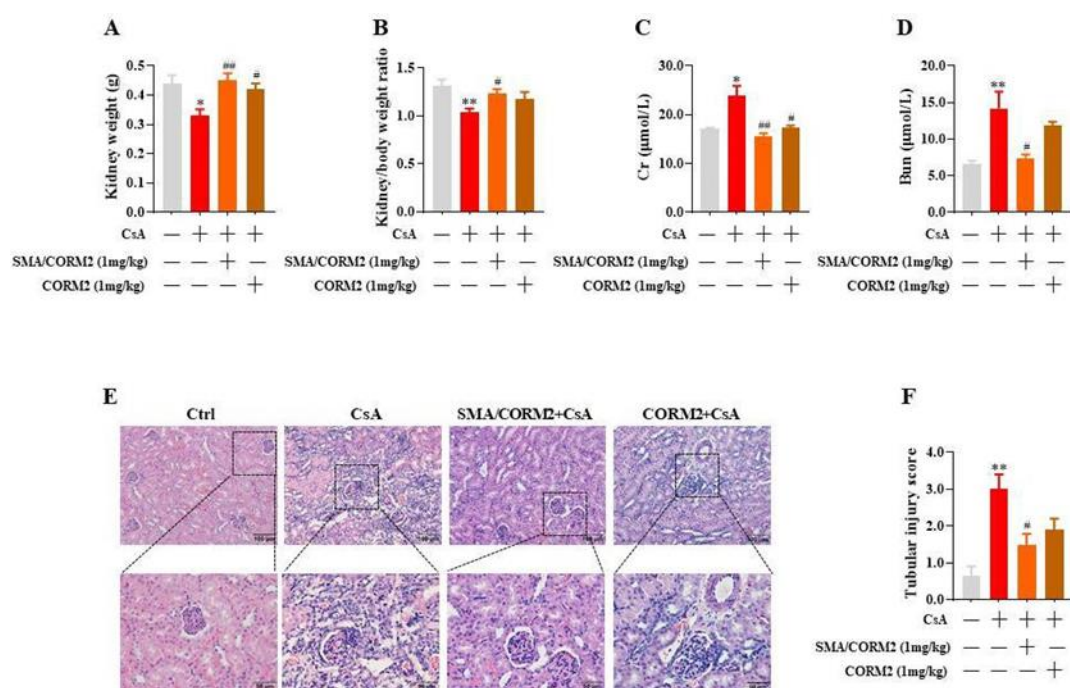


**Figure 2.** Renal pathological and histological changes after CsA treatment and the protective effect of SMA/CORM2 on renal injury. (A) Kidney weight 24 h after the last infusion of CSA, (B) Kidney/body weight ratio, (C) Serum creatinine, (D) blood urea nitrogen, (E) H&E staining for histological evaluation of the kidneys, (F) tubular injury score to evaluate the pathological changes of the kidneys. \* $P < 0.05$ , \*\* $P < 0.01$  vs control group; # $P < 0.05$ , ## $P < 0.01$  vs CsA group. The results were expressed by mean  $\pm$  standard error,  $n \geq 4$ .

### 3.2. CO content in different tissues after SMA/CORM2 treatment

To further confirm whether the protective effect of SMA/CORM2 is caused by CO and to verify its slow release and high bioavailability, we examined the rate of release of CO of SMA/CORM2 in different solvents under different conditions. As shown in **Figure 3A**, when SMA/CORM2 was dissolved in PBS with DMSO as the solvent, less than 10% of CO was released at 48 h. Within 2h after the 48 h, SMA/CORM2 had released more than 80% of CO. When SMA/CORM2 was dissolved in tissue homogenates or serum, the release of CO increased slightly (~20%) within 24 h. The release of CO within 48 h reached 60%–80%, which was consistent with our previous studies. This confirmed that the formation of SMA/CORM2 micelles can ensure the slow and stable release of CO. Next, we examined the distribution of CO *in vivo* after SMA/CORM2 intervention in a CsA-induced renal fibrosis model. As shown in **Figure 6B**, the amount of CO in the CsA-treated mice was slightly higher than that in the control group, which was due to the upregulation of HO-1 during validation. In addition, SMA/CORM2 treatment increased the concentration of CO in serum *in vivo*, and increased CO was also found in kidney tissues and increased CO in liver tissues, but no significant difference was found (FIG. 3B). In summary, SMA/CORM2 can target the accumulation of CO in inflammatory tissues and release CO, thus playing a protective role in injured tissues.

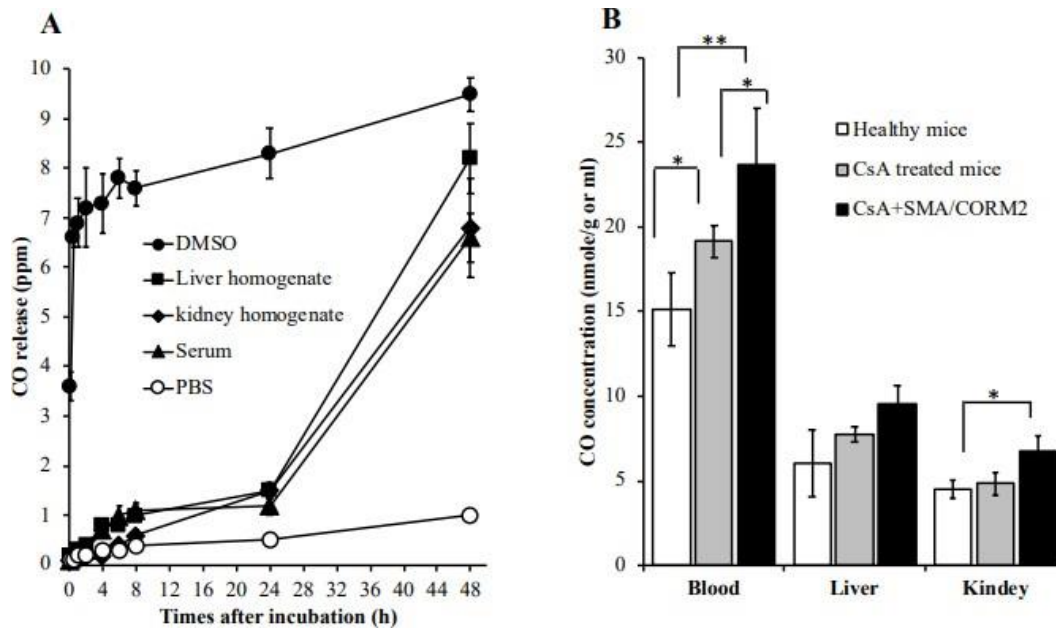


**Figure 3.** The amount of CO in different tissues after SMA/CORM2 treatment. (A) CO release; SMA/CORM2 was dissolved in different solvents and CO release was measured using gas chromatograph. (B) CO concentration; CsA-induced renal fibrosis model mice were killed 24h after the last injection of CsA. Blood and liver and kidney tissues were collected, 0.4ml PBS was added to every 100 mg of tissue, homogenized by a homogenizer, 0.5ml homogenated tissue and 0.2ml saponin were taken, incubated at room temperature for 24h, and then detected by gas chromatography for quantitative analysis. The control group was the content of CO in normal healthy mouse tissues. SMA/CORM2 alleviates CSA- induced renal fibrosis by inhibiting TGF- $\beta$ /Smad signaling pathway. \* $P < 0.05$ , \*\* $P < 0.01$  vs control group; # $P < 0.05$ , ## $P < 0.01$  vs CsA group. The results were expressed by mean  $\pm$  standard error,  $n \geq 4$ .

Based on the relief of renal toxicity and kidney injury caused by CsA by SMA/CORM2, we will focus on the influence of SMA/CORM2 on CSA-induced renal fibrosis and its mechanism in the following studies. As shown in **Figure 4A-B**, the results of Masson staining showed significant deposition of collagen fibers in the kidney of mice treated with CsA, while SMA/CORM2 intervention significantly reduced the area of renal fibrosis. The protein levels of  $\alpha$ -SMA and Col, typical markers of renal fibrosis, were significantly increased after CsA treatment, while SMA/CORM2 almost completely suppressed this trend (**Figures 4C, 4G, and 7H**), which were consistent with the results of Masson staining. In terms of its mechanism, we focused on the TGF- $\beta$ /Smad signaling pathway and detected the protein levels of TGF- $\beta$ 1, p-Smad2/3, and Smad2/3 in the renal tissue. The results showed that TGF- $\beta$ 1 and p-Smad2/3 protein levels significantly increased after CsA treatment, while SMA/CORM2 intervention significantly inhibited this trend (**Figure 4C-F**). These results suggest that the TGF- $\beta$ /Smad pathway is a potential mechanism by which SMA/CORM2 inhibits CsA-induced renal fibrosis.

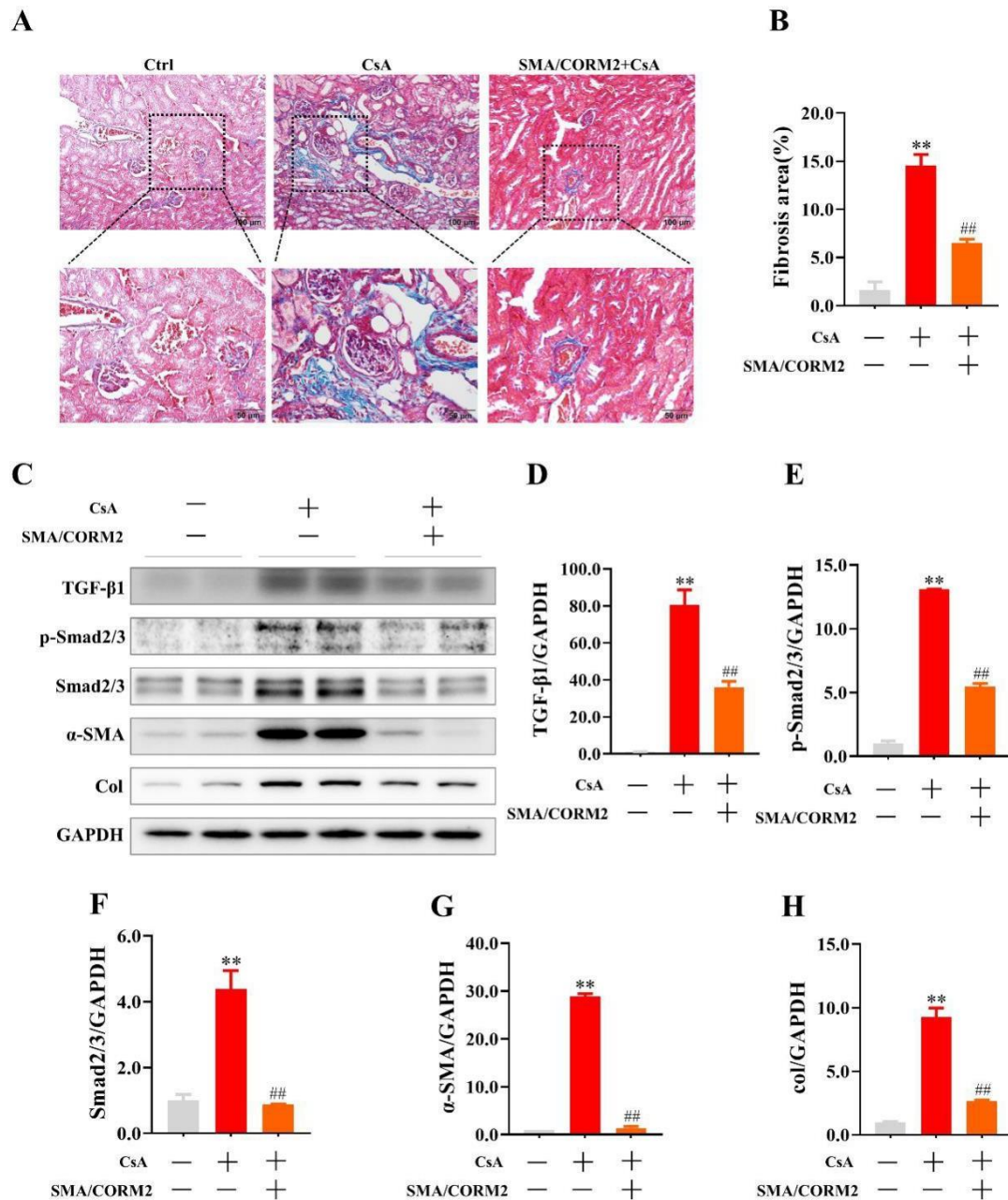


**Figure 4.** SMA/CORM2 alleviates CsA-induced renal fibrosis by inhibiting TGF- $\beta$ /Smad signaling pathway. (A) Collagen fiber deposition was observed by Masson staining of renal tissue to assess the degree of renal fibrosis, (B) Quantification of renal fibrosis area, (C) TGF- $\beta$ /Smad signaling pathway and fibrosis-related protein expression, such as TGF- $\beta$ 1, p-Smad2/3, Smad2/3,  $\alpha$ -SMA and Col, (D–H) quantitative analysis results. \* $P < 0.05$ , \*\* $P < 0.01$  vs control group; # $P < 0.05$ , ## $P < 0.01$  vs CsA group. The results were expressed by mean  $\pm$  standard error,  $n \geq 4$ .

#### 4. Discussion

Renal fibrosis is the destruction of renal structure and function caused by various reasons, which leads to the instability of renal structure, abnormal accumulation of extracellular matrix, and the production of a large amount of fibrotic protein, and ultimately leads to the loss of renal function and irreversible end-stage renal failure. The *NLRP3* inflammasome is a pattern recognition receptor whose membrane receptors are activated by the intracellular serine protease. Serine protease activator 1 can promote the expression of serine protease activator 3 in the nucleus, thereby inhibiting its activity and thus playing an anti-inflammatory role. Mas1 also binds to the serine protease activator 1 receptor to play an anti-inflammatory role. Therefore, activation of *NLRP3* inflammasome is an important cause of renal inflammatory response

and renal fibrosis, which means that blocking the activation of *NLRP3* inflammasome can effectively relieve the CsA-induced renal fibrosis.

One of the key issues in drug development is the targeted delivery of the active ingredient of the drug to the diseased tissue (API). In many targeted studies, nanomaterials based on the enhanced permeability and retention effect (EPR effect) in the inflammatory tissue have received much attention and are considered as a valuable research method [6,7]. EPR effect is a common phenomenon in tumor and inflammatory tissues. Compared to normal blood vessels, the blood vessels in tumors and inflammatory tissues have higher vascular permeability. Therefore, macromolecules with molecular weight greater than 40–50 kDa or nanomaterials larger than 5–10 nm cannot pass through normal tissues but can accumulate in the blood vessels of tumors and inflammatory tissues. This phenomenon is called “passive targeting.” So far, the EPR effect has been demonstrated not only in animal tumors, but also in human tumors. Based on this property of EPR effect, many nanodrugs, especially anti-cancer nanodrugs targeting tumors, have been developed, some of which have been approved and applied clinically, while others are still undergoing clinical trials. Although most studies based on the EPR effect are focused on cancer, we should also note that inflammatory tissue has similar properties to tumor blood vessels. In fact, the EPR effect was discovered by studying bacterial infections, so targeted nanomaterials using the EPR effect could also be applied to inflammatory diseases [8-10]. In our previous studies, we found the therapeutic potential of nano-designed drugs in inflammatory diseases, including colitis induced by sodium glucoside sulfate (DSS) in mice, repeated perfusion loss in liver ischemia, hypertension, and acetaminophen (APAP) induced liver injury [10-15].

## 5. Conclusion

This study found that the nano-sustained-CO releasing molecule (CS-CO) has a strong protective effect on the kidney; HK-2 cells and RTECs were treated with siRNA and inhibitors in *NLRP3* knockout mice, and the changes in cell activity and expression of intracellular inflammatory factors were detected. The expression of TGF- $\beta$ 1/Smad signaling pathway related proteins in HK-2 cells and RTECs were detected by ELISA, western blot, immunofluorescence, and other techniques.

## Funding

This project was funded by Health Commission of Hebei Province Chuanxiong: Extract Improves Inflammatory Response in Rats with Pyelonephritis through IL-6/STAT3 Signaling Pathway (Project number: 20231486)

## Disclosure statement

The authors declare no conflict of interest.

## References

- [1] Tian RF, Li PS, 2022, IFN- $\gamma$  Combined with TNF- $\alpha$  Stimulates Mesenchymal Stem Cells to Relieve Cisplatin- Induced Renal Fibrosis. *China Science and Technology Papers Online Quality Papers*, 15(03): 318–327.
- [2] Jiang Y, 2022, Coenzyme Q10 Inhibits Rip1-RIP3-MLK 1- Mediated Necrotic Apoptosis Through Wnt3 $\alpha$ / $\beta$ -catenin/GSK-3 $\beta$  Signaling Pathway to Reduce Renal Fibrosis in Rats with Unilateral Ureteral Obstruction, dissertation, Yanbian University.
- [3] Yuan Y, 2022, Study on the Mechanism of Action of Wenyang Zhenshuai Granules on Renal Fibrosis

Based on NLRP3 Inflammasome Mediated Pyrodeath, dissertation, Hunan University of Chinese Medicine.

- [4] Song G, He J, 2022, Research Progress of SIRT6 and the Mechanism of Diabetic Nephropathy. *Chin J Clinical Research*, 35(05): 717–720.
- [5] Zhou W, 2022, CircPlekha7 Targets miR-493-3p/KLF4 To Inhibit Renal Fibrosis, dissertation, Nanchang University.
- [6] Wallace JL, Vaughan D, Dicay M, et al., 2018, Hydrogen Sulfide-Releasing Therapeutics: Translation to the Clinic, *Antioxid Redox Signal* 28(16): 1533–1540.
- [7] Abraham NG, Kappas A, 2008, Pharmacological and Clinical Aspects of Heme Oxygenase. *Pharmacol Rev*, 60(1): 79–127.
- [8] Boczkowski J, Poderoso JJ, Motterlini R, 2006, CO-Metal Interaction: Vital Signaling from a Lethal Gas, *Trends Biochem Sci* 31(11): 614–621.
- [9] Ghosh S, Gal J, Marczin N, 2010, Carbon Monoxide: Endogenous Mediator, Potential Diagnostic and Therapeutic Target, *Ann Med* 42(1): 1–12.
- [10] Shao L, Liu C, Wang S, Liu J, et al., 2018, The Impact of Exogenous CO Releasing Molecule CORM-2 on Inflammation and Signaling of Orthotopic Lung Cancer, *Oncol Lett* 16(3): 3223–3230.
- [11] Zhang W, Tao A, Lan T, et al., 2017, Carbon Monoxide Releasing Molecule-3 Improves Myocardial Function in Mice with Sepsis by Inhibiting NLRP3 Inflammasome Activation in Cardiac Fibroblasts, *Basic Res Cardiol*, 112(2): 16.
- [12] Foresti R, Bani-Hani BG, Motterlini R, 2008, Use of Carbon Monoxide as a Therapeutic Agent: Promises and Challenges, *Intensive Care Med*, 34(4): 649–658.
- [13] Nagao S, Taguchi KH, Sakai R, et al., 2014, Carbon Monoxide-Bound Hemoglobin-Vesicles for the Treatment of Bleomycin-Induced Pulmonary Fibrosis, *Biomaterials* 35(24): 6553–6562.
- [14] Chaves-Ferreira M, Albuquerque IS, Matak-Vinkovic D, et al., 2015, Spontaneous CO Release from Ru(II)(CO)<sub>2</sub>-Protein Complexes in Aqueous Solution, Cells, and Mice, *Angew Chem Int Ed Engl* 54(4):1172–1175.
- [15] Santos-Silva T, Mukhopadhyay A, Seixas JD, et al., 2011, CORM-3 Reactivity Toward Proteins: The Crystal Structure of a Ru (II) Dicarbonyl-Lysozyme Complex, *J Am Chem Soc* 133(5): 1192–1195.

**Publisher's note**

Bio-Byword Scientific Publishing remains neutral with regard to jurisdictional claims in published maps and institutional affiliations.